PHYSICAL REVIEW B VOLUME 1, NUMBER 11 1 JUNE 1970

Crystal-Field Spectra of the Compensated Lattice: Nonlinear Magnetic Field Dependence and Polarization of Tetragonal Sm^{2+} Fluorescence in KCl†*

Francis K. Fong and James C. Bellows
Department of Chemistry, Purdue University, Lafayette, Indiana 47907
(Received 2 January 1970)

The field dependence and the polarization of the Zeeman components of 4.2 K fluorescence lines arising from Sm^{2+} ions in tetragonal compensation in KCl have been measured with magnetic fields up to 93.5 kG. The difficulties encountered in the interpretation of crystal-field spectra in lattices distorted by the presence of compensation defects are described. It has been concluded that all the observed narrow lines originate from the $^5D_0$ level, and that most probably the tetragonal lines arise from transitions in the Sm^{2+}-K^+ vacancy $C_{4v}(2,0,0)$ pair and the Sm^{2+}-O^{2-} $C_{4v}(1,0,0)$ pair. Representation origins of the observed lines have been determined from the polarization data, the field dependence of line intensities, and the previously determined Zeeman anisotropy fluorescence patterns.

I. INTRODUCTION

The interpretation of crystal-field spectra of ions is faced with three problems: (1) The site-symmetry origin of the transition in question, (2) the transformation properties of the initial and final states involved in the transition, which characterize the irreducible representations to which these states belong, and (3) the dipole origin of the transition in question. When the ion assumes a unique site symmetry, straightforward interpretation is usually possible. However, if the ion can assume several sites in a host lattice, as do trivalent lanthanide ions in alkaline-earth halides or divalent lanthanide ions in alkali halides, the problem becomes very complicated indeed. These ions usually enter the host lattice accompanied by compensation defects characteristic of the host. For example, the trivalent ions are compensated by anion interstitials in alkaline-earth halides, while the divalent ions in alkali halides are compensated by cation vacancies. Not only different types of site symmetries can exist; there are several possible sites corresponding to the same symmetry type. Moreover, there is always the possibility of charge compensation by divalent impurity anions. As a result, the spectra of ions in compensated lattices are often composite spectra of the various sites belonging to different or similar symmetry types that are consistent with the structure of the host lattice. In the following, the problems associated with the interpretation of crystal-field spectra in compensated lattices will be exemplified by Zeeman fluorescence spectra of the KCl: Sm^{2+} system, in which the K^+ vacancies provide for the necessary charge compensation of the Sm^{2+} ions, if the Cl^- sublattice is free of impurity divalent anions such as O^{2-} ions which can compete with the K^+ vacancies in the compensation of the Sm^{2+} ions.

The observation of Zeeman anisotropy fluorescence (ZAF) patterns characteristic of different site symmetries of Sm^{2+} in KCl was shown to be consistent with the pairing of the Sm^{2+} and K^+ vacancies along different crystal axes through a Maxwell-Boltzmann distribution that is governed by the geometric restrictions of the fcc lattice of KCl.[1–5] It was concluded[2,3] that the most dominant sites in the KCl:Sm^{2+} system are, in the order of their relative importance, the $C_{4v}(2,0,0)$, $C_s(2,1,1)$, $C_{2v}(1,1,0)$, and $C_1(3,2,1)$ sites, where the indices in parentheses denote the position of the vacancy in the K sublattice with Sm^{2+} at (0, 0, 0).[2] The spectra arising from transitions between the ^5D and ^7F multiplets are thus observed to be a superpositon of spectra characteristic of the different sites. The present paper reports the initial effort in the investigation into the site and representation origins of the lines in terms of field dependence and the polarization properties of the Zeeman components.

II. DEFINITION OF PROBLEM

While the site origins of practically all dominant lines have been determined through the ZAF patterns,[1–5] the detailed analysis of the representation origin of each fluorescence line remains a practically impossible task in the absence of some additional experimental handle. One difficulty lies in the fact that lines of the same site-symmetry origin can arise not only from sites of the same symmetry which differ only in the position of the K^+ vacancy relative to the Sm^{2+} ion, but also from transitions between different J levels which occur in overlapping energy regions. For example, lines arising from the (2, 0, 0) site

and the (4, 0, 0) site will both give rise to C_{4v} ZAF patterns. On the other hand, while many of the transitions in KCl:Sm^{2+} must initiate from the $^5D_0$ level, there remains the possibility that the $^5D_1$ level could also contribute to radiative decay of the electronically excited ions. The possibility of impurity anion (such as O^{2-}) compensation provides still a further complication of the problem.

The difficulty of interpretation of the spectral lines is exemplified by the no-field lines observed in the 8132.6–8204.9 Å region. Under an external magnetic field, these lines give rise to ZAF patterns that are characteristic of C_{4v} site origin. The patterns arising from the no-field lines at 8194.7, 8202.3, 8203.1, and 8204.9 Å overlap, which at first sight give the appearance of three identical E patterns with the corresponding apparent g factors of 5.04, 5.34, and 5.50, respectively.[1] In this view, the overlapping ZAF patterns are thought to arise from the transition between the $^5D_0$ level and the same E representation in the $^7F_4$ level in three different C_{4v} sites with the K^+ vacancy located at the (2, 0, 0), (4, 0, 0), and (6, 0, 0) lattice points in the K sublattice. Such an interpretation can now be critically assessed in light of recent findings from this laboratory.[2] The relative probabilities of finding the first three nearest C_{4v} sites according to an idealized Maxwell-Boltzmann distribution calculation[2] are, respectively, 7.7×10^{-1}, 1.1×10^{-4}, and 4.5×10^{-6} at 300 K. The population of these three tetragonal sites thus decreases by more than five orders of magnitude, which raises several questions concerning the spectral intensities of the overlapping patterns if the above interpretation is valid.

Another difficulty lies in the assumption that first-order Zeeman effects are observed only in the case when the E representation is involved.[1] This is true in the $S=1$ representation[1] when the cubic field is large compared with the axial field arising from the C_{4v} compensation. A comparison of theoretical ZAF patterns calculated through the idealized $S=1$ representation with the experimental ZAF pattern arising from the no-field line at 8194.7 Å reveals a serious discrepancy in that the splitting about the no-field line with $\vec{H}\parallel[100]$ is not equal. The departure from the ideal $S=1$ pattern could result from interaction of Zeeman components from two different E representations, in which case we should observe corresponding nonlinear field dependence of the Zeeman components with $\vec{H}$ along the C_4 axis. Not previously considered is the possibility that the axial field due to the compensation is not small compared with the cubic fields of the six Cl^- ligands, in which case the $S=1$ representation is no longer valid. In the following, the problems raised in this section will be dealt with in detail.

III. EXPERIMENTAL PROCEDURE

KCl crystals containing 3.6×10^{18} Sm^{2+} ions cm^{-3} were grown by the Czochralski method.[6] The rare-earth content was determined by an EDTA (ethylene diamine tetracetic acid) analysis. The 4.2 K spectra were recorded on Kodak photographic N plates with a 2-m Bausch and Lomb grating (4 in. ×4 in., 15 000 per in.) spectrograph and a 3 m Baird Associates grating (2 in. ×5 in., 15 000 per in.) spectrograph. In the low-field region, the magnetic fields were obtained with a Varian Associates 12-in. magnet with a $1\frac{1}{4}$-in. gap. The magnetic fields were calibrated with an Alpha Scientific Laboratories Model 610 Digital Gaussmeter. The maximum field in this case is 25.7 kG. In the course of our investigation, it became clear that in order to clear up some aspects of the problem described in Sec. II, it was desirable to extend our studies to higher magnetic fields. The high-field experiments were carried out at the Francis Bitter National Magnet Laboratory, where fields up to 215 kG are available. Because an optical access perpendicular to the magnetic field was necessary, however, the maximum field employed in the present investigation was limited to 93.5 kG. The fluorescence spectra in both cases were calibrated by iron arc and hollow cathode iron lamp spectra, the results being reproducible to an average deviation of 0.1 Å in most cases. Polarization studies were made with Wollaston-type and Nicol-type prisms. The propagation vector of the recorded fluorescence was directed along the [010] axis with the magnetic field vector, $\vec{H}$, in the [100] direction. Absorption spectra of the KCl:Sm^{2+}

TABLE I. Wavelengths, relative intensities, representation assignments, and number of Zeeman components ($\vec{H}\parallel[100]$) of the tetragonal Sm^{2+} $0\rightarrow4$ no-field 4.2 K fluorescence lines.

Line	λ(Å)	Relative intensity[a]	Assignment[b]	Zeeman components
I	8204.9	10.0	$A_1\rightarrow A_1$	2
II	8203.1	<0.1	$A_1\rightarrow E$	4
III	8202.3	<0.1	$A_1\rightarrow E$	4
IV	8194.7	3.5	$A_1\rightarrow A_2$	2
	(~8194)[c]		$A_1\rightarrow A_1$	2
V	8132.6	0.7	$A_1\rightarrow A_2$	2

[a]Integrated intensity relative to the most intense no-field line observed for the $0\rightarrow4$ transitions as given by Bron and Heller (Ref. 15).

[b]Assignment of the representation origins of the fluorescence line has been made in Sec. IV D.

[c]The line at ~8194 Å ($A_1\rightarrow A_1$) is not observed. Its existence is manifested by the Zeeman components which arise from it under $\vec{H}\parallel[100]$ (Secs. IVC, IVD).

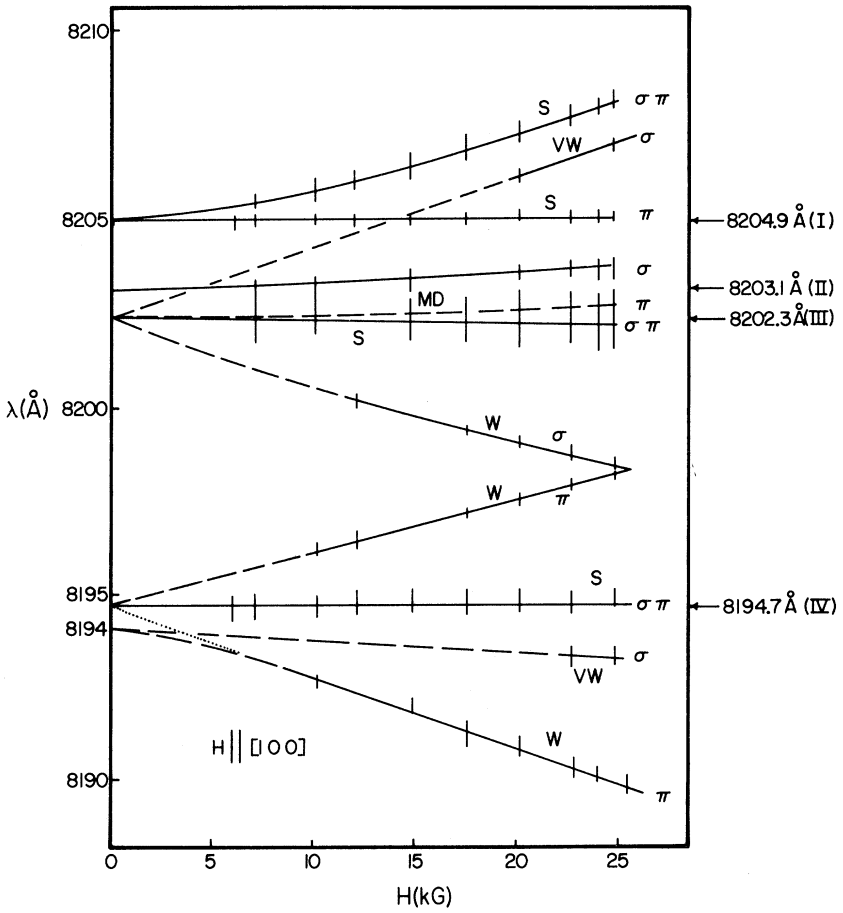

FIG. 1. Field dependence up to 25.7 kG ($\vec{H} \| [100]$) of the Zeeman components of the no-field lines I, II, III, and IV, along with the polarizations. Intensities are indicated by: S means strong; M means medium; W means weak; VW means very weak. D means diffuse. Dashed lines indicate extrapolations to zero field (see Sec. IV D). The dotted line shows linear extrapolation to zero field of the lowest π component as if it originated from IV.

sample were measured at 4.2 and 77 K with a Cary 14H spectrophotometer. The temperature dependence of the first band corresponding to transitions between the $4f^6$ and $4f^5 5d^1$ configurations was recorded.

IV. EXPERIMENTAL RESULTS AND INTERPRETATIONS

The observed 4.2 K fluorescence lines I to V in the 8132 – 8205 Å wavelength region, along with their relative intensities, are listed in Table I. The ZAF patterns, at 26.5 kG with $\vec{H}$ rotating in the (001) and (01$\bar{1}$) planes, which arise from the no-field lines have been shown previously.[1,3] In view of these earlier ZAF determinations, all the lines listed in Table I have been shown to arise from tetragonal Sm^{2+} site symmetries. The field dependence of the Zeeman components of the no-field lines I–IV (Table I) up to 25.7 kG with $\vec{H} \|$ [100] axis is shown in Fig. 1. The polarizations of the Zeeman components are also shown, with σ denoting $\vec{E} \perp \vec{H}$ and π denoting $\vec{E} \| \vec{H}$. The combined notation $\sigma\pi$ denotes the case in which both the σ and π components are simultaneously observed, with the σ component being the stronger. The Zeeman components arising from the no-field lines II and III are not resolved at low fields. The most important feature of Fig. 1 is that for H up to 25.7 kG, the two Zeeman components of the ZAF pattern arising from IV [Fig. 7(a) of Ref. 1] show a linear dependence on the magnetic field strength. The linearity in the field dependence in this case clearly rules out the possibility of interaction between two E representations as an explanation for the observed departure from the ideal $S = 1$ representation (Sec. II).

The field-dependence measurements at high fields are shown in Fig. 2. There are 2, 4, 4, 4, and 2 components for the zero-field lines I, II, III, IV, and V, respectively. With $\vec{H} \|$ [100], the tetragonal site whose C_4 axis is along the [100] axis will assume a C_4 symmetry. On the other hand, the two equivalent sites whose C_4 axes lie along the [010] and [001] directions will assume a C_s site symmetry. The no-field singlet line must therefore give rise to two components corresponding to the two new site symmetries created by the presence of the external field. By the same argument, the no-field line which gives rise to four

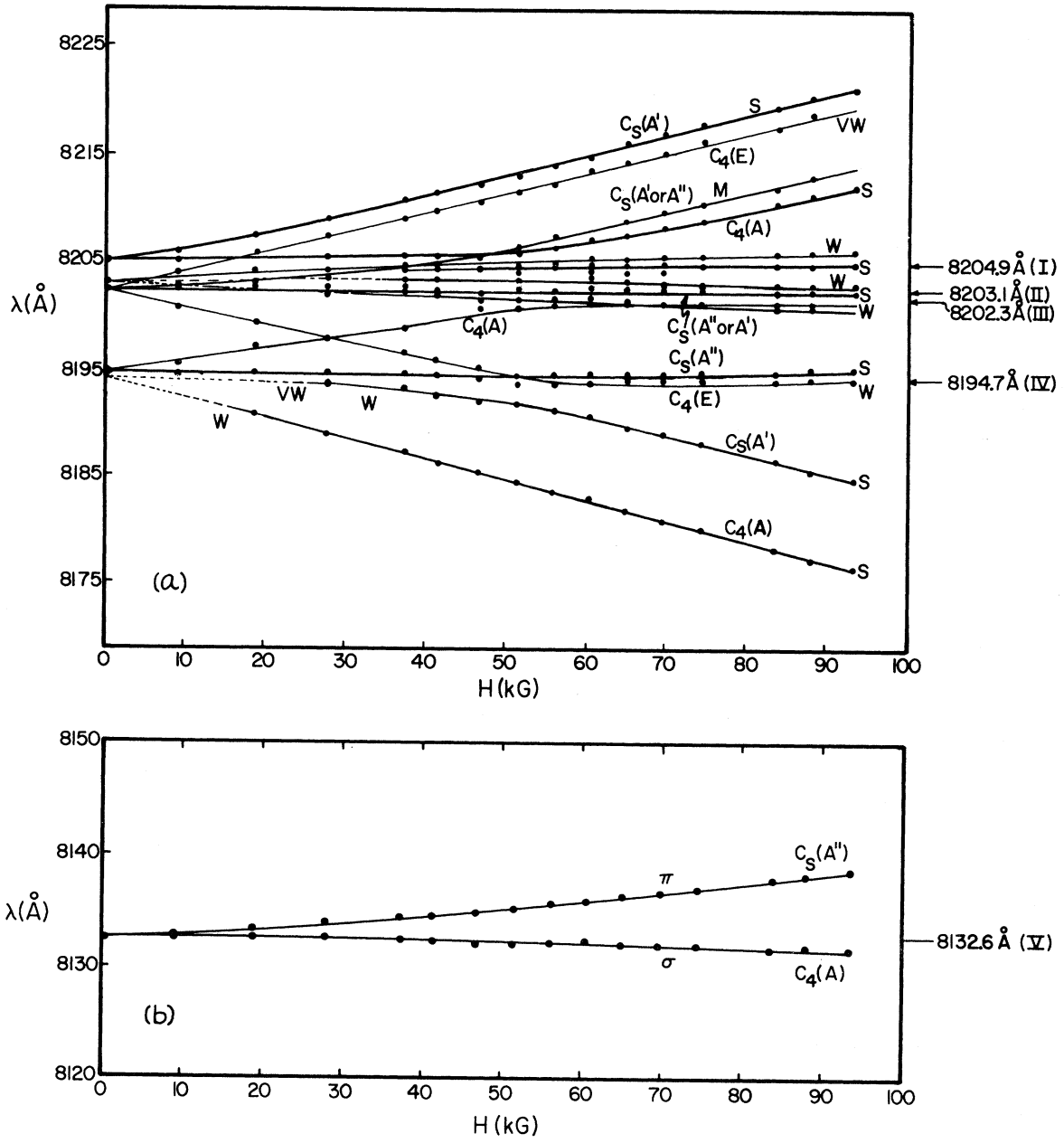

FIG. 2. Field dependence up to 93.5 kG ($\vec{H} \| [100]$) and site-symmetry origin of the Zeeman components of (a) the no-field lines I, II, III, and IV and (b) the no-field line V. The four components of II and the two C_s components of III are not easily distinguishable. The site-symmetry assignment of the Zeeman components is discussed in Sec. IV D.

components with $\vec{H} \| [100]$ must correspond to a no-field line that is a doublet.

The temperature dependence of the $4f^6 \rightarrow 4f^5 5d^1$ band is shown in Fig. 3, along with the corresponding position of the observed $^5D_0$ level and that expected for $^5D_1$. This information is important in our discussion concerning the role of $^5D_1$ as an initial level in transitions to the ground ^7F multiplet, as well as the sharp temperature dependence of the $^5D_0 \rightarrow {}^7F_J$ transitions.

A. Weak Axial Field Case

In the $S=1$ representation, we write for the effective Hamiltonian[1]

$$\mathcal{H}_{eff} = \beta \vec{H} \cdot \overleftrightarrow{g} \cdot \vec{S} + D[S_z^2 - \tfrac{1}{3} S(S+1)] \quad , \qquad (1)$$

where β is the Bohr magneton, $\overleftrightarrow{g}$ is a second-rank tensor, and $\vec{S}$ is the effective angular momentum vector. It was assumed that the cubic crystal field was much larger than the charge compensa-

tion field. Under this assumption, the $S=1$ representation can be meaningfully employed since only the threefold degenerate T_1 and T_2 representations need be considered for first-order Zeeman effects. The second term in Eq. (1) effectively splits the 3-dimensional T_1 and T_2 cubic representations into A_2+E and B_2+E representations of C_{4v}, respectively. The solution of the 3-dimensional matrix equation, however, seriously disagrees with the experimental finding in that the observed Zeeman components at 26.5 kG when $\vec{H}$ is parallel to [100] are not symmetrically displaced about the no-field line. It was suggested[1] that the discrepancy could be the result of higher-order interaction resulting from nontrivial matrix elements connecting states from two different E representations. An unambiguous test of such a possibility is afforded by an investigation into the field dependence of the Zeeman components. In a magnetic field there are three distinguishable C_{4v} sites with the C_4 axes along the [100], [010], and [001] directions, respectively. If the Zeeman effect is small compared with the crystal Stark splittings, the Zeeman splitting of the E representation will be linear with the magnetic field strength. At sufficiently high magnetic field strength, nondiagonal matrix elements connecting states of different E representations become important as nonlinear Zeeman effects become pronounced. Departure from the ideal $S=1$ representation could thus be accounted for.

B. Determination of Dipole Origin from Polarization

The above phenomenon, however, is not observed. The field dependence up to 25.7 kG of the Zeeman effect associated with the 8194.7 Å no-field line (IV) is clearly linear (Fig. 1). For a reassessment of the situation, we consider the polarizations of the Zeeman components in Fig. 1. With $\vec{H} \parallel [100]$, the site symmetry of the C_{4v} [100] site is reduced to C_4, whereas that of the C_{4v}[010] and C_{4v}[001] sites is reduced to C_s. If we (1) choose $\vec{H} \parallel [100]$ to be the z axis, (2) assume that the initial state in the dipole transition moment to be either $A_1(^5D_0)$ or $A_2(^5D_1)$, [7] and (3) remember that the fluorescence is viewed in a direction perpendicular to $\vec{H}$, we make the following observations. Consider the case when the no-field final states belong to a C_{4v} E representation. For the C_{4v} [100] site in a magnetic field $\vec{H} \parallel [100]$, the nonvanishing matrix elements are $\langle A_i | x - iy | E_f \rangle(\sigma)$ $\langle A_i | x + iy | E_f \rangle(\sigma)$, $\langle A_i | L_x - iL_y | E_f \rangle(\pi)$, and $\langle A_i | L_x + iL_y | E_f \rangle(\pi)$, where i and f denote the initial and final states, respectively. This is true whether the initial no-field state is an $A_1(^5D_0)$ state or an $A_2(^5D_1)$ state in C_{4v}, since in either case the initial state would transform as an A representation in the C_4 symmetry. The resulting fluorescence lines will thus be σ polarized for an electric dipole (the components of which transform as x, y, and z), and π polarized for a magnetic dipole (the components of which transform as L_x, L_y, and L_z). If the no-field final states belong to the C_{4v} A_1 and A_2 representations,[8] the nonzero matrix elements in a magnetic field $\vec{H} \parallel [100]$ are $\langle A_i | z | A_f \rangle(\pi)$ and $\langle A_i | L_z | A_f \rangle(\sigma)$. The resulting fluorescence lines in this case will be π polarized for an electric dipole and σ polarized for a magnetic dipole. For the C_{4v}[010] and C_{4v}[001] sites, the $\vec{H} \parallel [100]$ field lowers the site symmetry to C_s. If the no-field final states were E states, in C_s symmetry they would transform under the A' and A'' representations, which would be indistinguishable from A_1 and A_2 states which also transform as A' and A'',

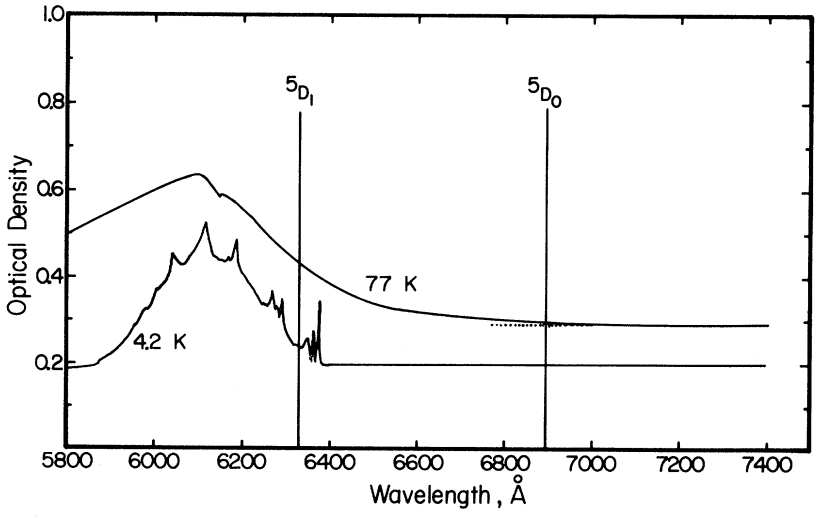

FIG. 3. First $4f^6 \rightarrow 4f^5 5d^1$ absorption band in KCl:Sm^{2+} at 4.2 and 77 K along with the expected $^5D_0$ and $^5D_1$ levels of the $4f^6$ configuration in Sm^{2+}.

respectively, in C_s. The nonvanishing matrix elements are $\langle A_i' | x, y | A_f' \rangle(\sigma)$, $\langle A_i' | L_z | A_f' \rangle(\sigma)$, $\langle A_i' | z | A_f'' \rangle(\pi)$, and $\langle A_i' | L_x, L_y | A_f'' \rangle(\pi)$ if the no-field initial state is an A_1, and $\langle A_i'' | x, y | A_f'' \rangle(\sigma)$, $\langle A_i'' | L_z | A_f'' \rangle(\sigma)$, $\langle A_i'' | z | A_f' \rangle(\pi)$, and $\langle A_i'' | L_x, L_y | A_f' \rangle(\pi)$, if the no-field state is an A_2. Regardless of the dipole origin, there will be one π-polarized line and one σ-polarized line.

C. Strong Axial Field Case

The conclusion to be drawn from the above discussion is that unless the dipole origin is known, there is no way of attributing a given C_{4v} pattern to a no-field E representation or two closely spaced no-field A_1 and A_2 representations. Conversely, there is no way of determining the dipole origin of a given C_{4v} pattern unless we know the representation origin of the no-field lines. In the previous work,[1] the $S=1$ representation was assumed, and the E representation of the final states was presupposed. Under such assumptions, it was possible to determine the dipole origin of the anisotropy patterns. This was done in the cases of a C_{4v} pattern in $J=6$ and a C_{2v} pattern in $J=5$.[9] In view of our present discussion, however, it is clear that we must first establish either the representation of the no-field final states or their dipole origins before a meaningful analysis can be made.

That it is possible to have an A_1 state and an A_2 state closely spaced in a C_{4v} complex can be readily illustrated by the solution of the 9×9 matrix equation for $J=4$ employing the Hamiltonian

$$\begin{aligned}\mathcal{H} = {} & e\beta A_{40}\langle r^4\rangle\{[\,35J_z^4 - 30J(J+1)J_z^2 + 25J_z^2 \\ & - 6J(J+1) + 3J^2(J+1)^2] + (\tfrac{5}{56})^{1/2}[\,J_+^4 + J_-^4]\} \\ & - e\gamma A_{60}\langle r^6\rangle\{[\,231\,J_z^6 - 315\,J(J+1)J_z^4 + 735J_z^4 \\ & + 105J^2(J+1)^2J_z^2 + 525J(J+1)J_z^2 + 294J_z^2 \\ & - 5J^3(J+1)^3 + 40J^2(J+1)^2 - 60J(J+1)] \\ & - \tfrac{21}{4}[\,(11J_z^2 - J(J+1) - 38)(J_+^4 + J_-^4) \\ & + (J_+^4 - J_-^4)(11J_z^2 - J(J+1) - 38)]\} \\ & - e\alpha A_{20}\langle r^2\rangle[\,3J^2 - J(J+1)]\,, \end{aligned} \tag{2}$$

where α, β, and γ are operator equivalence factors.[10] The parameters A_{40} and A_{60} arise from the cubic field, and A_{20} is associated with the axial field from the compensation along the C_4 axis. For rare-earth ions, the term containing the parameter A_{60} usually cannot be neglected.[11] For the sake of simplicity, however, we set $A_{60}=0$. The solutions of the 9×9 matrix equations for $J=4$, as we vary the axial compensation field A_{20}, are shown in Fig. 4. We observe that as A_{20} increases, there are an A_1 state and an A_2 state approaching each other in energy. The same result is observed for values of $A_{60}\neq 0$. Clearly, at values of A_{20} at which the cubic field is of the order of, or is actually smaller than, the compensation field, the $S=1$ representation is not readily justified. Indeed, the linear field dependence of the C_4 Zeeman components of the no-field line IV (Fig. 1), the ZAF pattern of which does not fit the $S=1$ representation of an $A \rightarrow E$ transition, appears as strong evidence of the possibility that IV in fact corresponds to an $A_1(A_2)$ state in close proximity to an $A_2(A_1)$ state.

D. Assignment of Transitions

In the tetragonal site symmetry, the ninefold degeneracy of the $J=4$ level is split into the A_1, A_2, E, B_1, A_1, E, and B_2 irreducible representations of the C_{4v} point group. If the initial state is the ${}^5D_0$ level, transitions to the A states and the E states in the $J=4$ manifold of a single tetragonal site will give rise to a total of five lines of either electric or magnetic dipole origin. The B_1 and B_2 states will not give rise to dipole transitions of either type. For a single tetragonal site, we should expect a maximum of four electric dipolar lines ($A_1 \rightarrow 2A_1 + 2E$) for the $0\rightarrow 4$ (${}^5D_0 \rightarrow {}^7F_4$) transition. Similarly, there is a maximum of three no-field lines ($A_1 \rightarrow A_2 + 2E$) for magnetic dipole transitions.

Three complicating factors in the interpretation of the observed spectral lines are (1) the possible superposition of $1\rightarrow 6$ (${}^5D_1 \rightarrow {}^7F_6$) transitions, in which case the spectrum will become so complicated that no easy interpretation could be made, (2) the possible superposition of $0\rightarrow 4$ transitions arising from two tetragonal sites such as $C_{4v}(2, 0,$

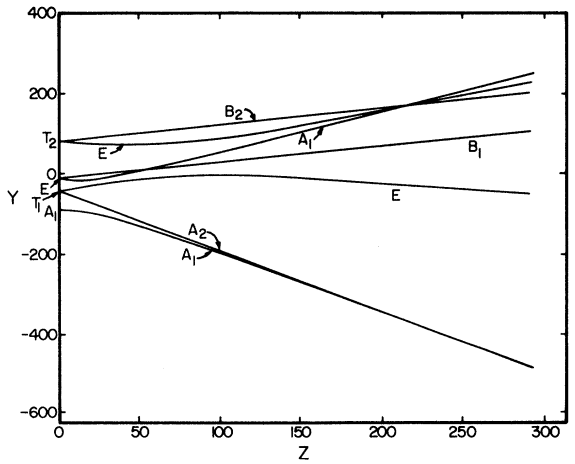

FIG. 4. Decomposition of the $J=4$ manifold employing Eq. (2), with $A_{60}=0$, and $Z=A_{20}\langle r^2\rangle/A_{40}\langle r^4\rangle$. Y is dimensionless. At $Z=0$, the eigenvalues correspond to irreducible representations of the cubic group.

0)and $C_{4v}(4,0,0)$, and (3) the possible superposition of transitions from vacancy compensated sites and those of anion impurity compensated sites. The first complication can be readily eliminated. Using energy levels for Sm^{2+} from the literature,[12] one finds that, while the $1\rightarrow6$ and $1\rightarrow5$ transitions occur in the vicinity of the $0\rightarrow4$ and $0\rightarrow3$ transitions, respectively, transitions $1\rightarrow4$ and $1\rightarrow3$ should occur between $0\rightarrow2$, $0\rightarrow1$, and $0\rightarrow0$ transitions, and $1\rightarrow2$, $1\rightarrow1$, and $1\rightarrow0$ transitions should occur at the high frequency side of the $0\rightarrow0$ transition. Since no fluorescence lines are observed other than the expected $0\rightarrow J$ transitions at approximate Landé intervals, transitions from the $^5D_1$ level, if they occur at all, apparently have nonvanishing transition moments *only* to the $^7F_6$ and $^7F_5$ manifolds for all the multiplicity of sites that exist in the compensated lattice. The conclusion that transitions originating from the $^5D_1$ level in fact are not observed, can be arrived at in terms of the following argument. From Fig. 3, we observe that the $^5D_1$ level lies 113 cm^{-1} above the onset of the $f^6\rightarrow f^5d^1$ band at 4.2 K. Since at $T=4.2$ K, $kT=2.9 cm^{-1}$, the population of the $^5D_1$ level, assuming Boltzmann statistics, is vanishingly small. Moreover, transitions from levels merged in the d band do not give rise to narrow lines which characterize the $f\rightarrow f$ transitions. In this direction, it is appropriate here to comment on the sharp temperature dependence of the $KCl:Sm^{2+}$ fluorescence. All the narrow fluorescence lines reported here and elsewhere[1,3-5] disappear at 77 K at which fluorescence is observed as a broad band spanning the entire wavelength region corresponding to the $0\rightarrow1-6$ transitions. The information given in Fig. 3 provides the reason for this temperature dependence: While at 4.2 K, $^5D_0$ is situated well below the d band, at 77 K it is located just above the onset of the temperature broadened d band.

Since by the above argument all the observed lines must originate from the $^5D_0$ level, we should expect only a *maximum* of five no-field lines arising from dipolar transitions to the $J=4$ manifold (i.e., $A_1\rightarrow2A_1+A_2+2E$). These five no-field lines will give a total of $2\times2+2+2\times4=14$ Zeeman components under $\vec{H}\parallel[100]$, if only one unique tetragonal site is responsible for the fluorescence lines. Since there are in all 16 components (Fig. 2) arising from the five observed no-field lines in the $0\rightarrow4$ wavelength region (Table I), we conclude that there must be at least two difference tetragonal sites that are responsible for the observed fluorescence. (The quadrupolar transitions in rare-earth ions are very weak compared with the dipolar transitions, and their occurrence is unlikely.) By virtue of statistical considerations,[2] the ratio of the most probable distribution numbers at 300 K for the $C_{4v}(2,0,0)$ site and the $C_{4v}(4,0,0)$ site is $\sim10^4:1$(Sec. II). Since the fluorescence intensity should be proportional to the concentration to a first approximation,[3] we rule out the possibility of superposition of lines due to contribution from the $C_{4v}(4,0,0)$ site. This line of argument leads us to the conclusion that, in addition to the $C_{4v}(2,0,0)$ Sm^{2+}-vacancy pair, a second tetragonal site which contributes to the fluorescence lines listed in Table I most probably arises from compensation of the Sm^{2+} ion by a dinegative anion located at a Cl^- site along a [100] axis. The most likely candidate for an unintentional impurity dinegative anion in the Cl^- sublattice is the O^{2-} ion. If this is true, the second tetragonal Sm^{2+} site is most probably the Sm^{2+} - O^{2-} $C_{4v}(1,0,0)$ pair.

With $^5D_0$ as the initial level, selection rules for magnetic and electric dipole transitions involving Zeeman components of C_{4v} A_1, A_2, and E final states can be readily deduced from the discussion in Sec. IV B. These selections are listed in Table II. By means of Table II, along with the observed polarizations, field dependence, and ZAF patterns, we now proceed to make assignments in the order of decreasing certainty for the tetragonal $0\rightarrow4$ lines. The π component of line V corresponds to the isotropic line in the ZAF pattern,[3] which means that it originates from the C_{4v} site under an $\vec{H}$ field perpendicular to its C_4 rotational axis. The reduced symmetry of the site in question is C_s. In this case, a π polarization will result for either dipole origin if and only if the final state is the A'' representation, which is derived from the no-field $C_{4v}A_2$ representation (Table II). The no-field line V is thus *unambiguously* determined to arise from $A_1(^5D_0)\rightarrow A_2(^7F_4)$ transition. Moreover, the σ polarization of the C_4 component clearly indicates its electric dipole origin.

In terms of the ZAF pattern, the two π components of line IV correspond to C_4 site under $\vec{H}\parallel[100]$,

TABLE II. Selection rule table for the polarization of Zeeman components ($\vec{H}\parallel[100]$) arising from tetragonal Sm^{2+} transitions originating from the $^5D_0(A_1)$ level. The notations σ and π are explained in the text.

No-field final state	Final state under $\vec{H}\parallel[100]$		Magnetic dipole	Electric dipole
	C_4	C_s		
A_1	A		σ	π
		A'	σ	σ
A_2	A		σ	π
		A''	π	π
E	E		π,π	σ,σ
		A'	σ	σ
		A''	π	π

while the σ and $\sigma\pi$ components of line IV correspond to C_s sites. The departure of the ZAF pattern of IV from the $S=1$ representation and the linearity of the field dependence of the C_4 components up to field strengths of ~27 kG suggests the A_1 and A_2 origins of the no-field lines involved (Sec. IV C). Substantiation of this statement can be made as follows. The C_4 components of IV are too weak to be observed at fields lower than ~15 kG (Fig. 1). However, their intensities increase with the applied field such that they become readily observable at fields above ~20 kG (Figs. 1 and 2). This field dependence of the line intensities can be interpreted in terms of the electric dipole origin of the C_4 components. The magnitude of the electric dipole transition moment depends on the admixtures of opposite parity states from the first excited configuration $4f^5 5d^1$. The external field, which lowers the C_{4v} site symmetry to C_4, effectively increases the importance of the odd-parity terms in the crystal-field potential expansion, thus increasing the electric dipole transition moments as previously discussed.[13] Thus the observed π polarization of the C_4 components of line IV must mean (according to Table II) that the corresponding no-field final states are an A_1 state and an A_2 state closely spaced in energy, only one of which is observed as IV in the absence of an external field. The σ component of IV arises from a C_s site under $\vec{H} \parallel [100]$, and is probably of electric dipole origin as it is not observed at fields lower than 22.5 kG (Figs. 1 and 2). This means that its C_{4v} representation origin is A_1 (Table II). According to such an assignment, therefore, the σ component and the lower π component of IV arise from the no-field line $^5D_0 \rightarrow A_1$, which is not observed. An extrapolation of the field dependence of these two components to $H=0$ yields a wavelength of 8194 Å for the $^5D_0 \rightarrow A_1$ transition, which is listed in Table I along with the observed lines. The $\sigma\pi$ line of IV and the upper π component belong to the no-fields $^5D_0 \rightarrow A_2$ transition in this analysis, except that only a pure π polarization (instead of the observed $\sigma\pi$) is allowed for the C_{4v} site reduced to C_s under $\vec{H} \parallel [100]$ for either an electric dipole transition moment or a magnetic dipole moment (Table II). The observation of a mixed polarization thus suggests a misalignment of crystal axes in our experiment, or an unaccounted for local distortion of site symmetry about the Sm^{2+} ion.

In the case of no-field line III, the σ components corresponding to the anisotropic lines in the ZAF pattern[1,3] (which arise from sites that are C_4 in symmetry when $\vec{H} \parallel [100]$) are probably of electric dipole origin in view of the field dependence of their intensities (see Figs. 1 and 2). On this basis, we are led to the conclusion that line III most probably arises from a $^5D_0 \rightarrow E$ transition (Table II). The C_s components of III are not clearly distinguishable from the four Zeeman components of II for a large part of the field-strength range employed.

The Zeeman components of II are not resolved at low fields (Fig. 1). At high-field strengths (Fig. 2) they are resolved, but the interpretation is complicated by the presence of the two C_s lines from III. If we assume that there are only two difference tetragonal sites that give rise to all the observed tetragonal lines I–V in the $0 \rightarrow 4$ region, the presence of four Zeeman components leads to the E origin of II. The four Zeeman lines of II cannot arise from two close by A_1 and A_2 states since both A_2 states (one from each of the two tetragonal sites) have already been accounted for in the preceding discussion. If this assignment is correct, lines II and III (both of E origins) must arise from different Sm^{2+} sites since the Zeeman components from two E representations of the same site must repel, contrary to the crossing patterns shown in Figs. 1 and 2.

Finally, the presence of two Zeeman components from the no-field line I indicates that I originates from either an A_1 state or an A_2 state. Since, by assumption, the two A_2 states are already accounted for, I must correspond to a $^5D_0 \rightarrow A_1$ transition. If we further assume that I and its Zeeman components are of electric dipole origin (which is reasonable in view of its high relative intensity as shown in Table I), the π component must correspond to the C_4 site (Table II). The mixed polarization $\sigma\pi$ of the remaining component (presumably the C_s component), as in the case of the $\sigma\pi$ line in IV, is perplexing since there should be only a pure σ polarization from the C_s site, regardless of the dipole origin. The lack of an isotropic line in the ZAF pattern[1,3] for line I deprives us of a definite assignment of the C_S (of the C_4) site symmetry under $\vec{H} \parallel [100]$. This lack somewhat weakens our case for the assignment of I.

V. DISCUSSION AND SUMMARY

In Sec. IV, we have established (i) that all the Sm^{2+} lines arise from the $^5D_0$ level, (ii) that *at least* two tetragonal sites are responsible for the observed lines, and (iii) that additional C_{4v} sites most probably arise from dinegative anion compensation since $C_{4v}(4,0,0)$ Sm^{2+}-K^+ vacancy pairs probably do not exist in sufficient numbers to give the observed intensities. The representation origins of the lines I–V have been determined. In the assignments of lines I and II, it was necessary to assume that *only* two different C_{4v} sites

are responsible for the observed tetragonal lines. The assumption that only two C_{4v} Sm^{2+} sites are important appears to be reasonable. We have excluded the $C_{4v}(4,0,0)$ Sm^{2+}-K^+ vacancy on grounds of statistical considerations. Compensation by a dinegative anion (presumably the O^{2-} ion) in the Cl^- sublattice can be the only other possibility which will give rise to C_{4v} compensation. The most stable Sm^{2+}-O^{2-} pair (assuming O^{2-} compensation) is probably the nearest-neighbor pair with O^{2-} at the (1, 0, 0) lattice point. The next-nearest C_{4v} Sm^{2+}-O^{2-} is the $C_{4v}(3,0,0)$ pair, which must be quite improbable statistically since in this case the distance of separation between the Sm^{2+} ion and the O^{2-} ion is three times that of the $C_{4v}(1,0,0)$ pair, assuming no lattice distortions are caused by the interaction of the Sm^{2+} and O^{2-} ions.

In the representation assignments, we have made use of the group-theoretical orthogonality theorems (Sec. IV B and Table II), the polarization data (Fig. 1), the field dependence of line intensities (Figs. 1 and 2), and the ZAF patterns determined previously[1,3] which can give unique information concerning the site origin of the Zeeman component: With $\vec{H} \parallel [100]$, the component corresponding to the isotropic line in the ZAF pattern must be of C_S origin, while that corresponding to the anisotropic line must be of C_4 origin.[1,14]

The nonlinear field dependence of the Zeeman components shown in Fig. 2 should provide us with a unique fit of the four parameters in an effective Hamiltonian containing the second-, fourth-, and sixth-order terms of the C_{4v} crystal-field potential and the Zeeman interaction term $g_\lambda \beta \vec{H} \cdot \vec{J}$ where $g_\lambda = 1.5$ is the Landé g factor, β is the Bohr magneton, and $\vec{J}$ is the total angular momentum operator. Such a fit represents a considerable effort in numerical analysis, which is underway at this laboratory.

Prior to our investigations, all the KCl:Sm^{2+} fluorescence lines discussed in the present paper were assigned to irreducible representations of the C_{2v} point group by Bron and Heller.[15] A nearest-neighbor Sm^{2+}- vacancy complex C_{2v} crystal-field Hamiltonian was obtained through a "fit" of their experimental data.[15] On the other hand, the crystal-field fluorescence spectra of trivalent lanthanide ions in CaF_2 have been interpreted in terms of the cubic field of the host without much consideration of the charge compensation F^- interstitial,[16] not to mention the possible occurrence of O^{2-} compensation which is known to exist.[17] In view of the present discussion, it appears certain that if line assignments are not made in terms of the site symmetries (through, for example, ZAF determinations), the polarizations, the dipole origins, and the field dependence of Zeeman components, any agreement between calculations and observed spectral lines of ions in compensated lattices must be fortuitous.

Finally, it is appropriate to mention an additional experiment we conducted which might give independent and further support of the role of O^{2-} ions in the compensation of the Sm^{2+} ions. Instead of the crystal preparation in which only $SmCl_3$ was employed[6] as the starting material, varying concentrations of Sm_2O_3 were added to the melt from which single crystals were grown. The resulting samples were then subjected to fluorescence spectroscopic analysis. No *additional* lines to those reported here and elsewhere were observed. The nonobservance of additional lines can only mean that the fluorescence lines due to O^{2-} compensation of the Sm^{2+} ions are already among the tetragonal lines observed in samples which were thought to be "oxygen free." While much detailed work is needed (such as comparison of the line intensities with O^{2-} concentration) in the investigation of the competitive processes of K^+ vacancy and O^{2-} compensation mechanisms, we are confident that the analysis given herein is conclusive.

---

†Research supported in part under the Advanced Research Projects Agency institutional Grant SD No. 102.

*Part of the experimental work reported in this paper was carried out at the Francis Bitter National Magnet Laboratory, which is supported by the U. S. Air Force Office of Scientific Research.

[1]F. K. Fong and E. Y. Wong, Phys. Rev. 162, 348 (1967).

[2]F. K. Fong, Phys. Rev. 187, 1099 (1969).

[3]F. K. Fong, R. H. Heist, C. R. Chilver, J. C. Bellows, and R. L. Ford, J. Luminescence 1, 889 (1970).

[4]F. K. Fong, Phys. Rev. (to be published).

[5]F. K. Fong and J. C. Bellows, Phys. Rev. (to be published).

[6]F. K. Fong, J. A. Cape, and E. Y. Wong, Phys. Rev. 151, 299 (1966).

[7]Both $^5D_0 \rightarrow {}^7F_4$ and $^5D_1 \rightarrow {}^7F_6$ transitions are considered since they would both occur in the same wavelength region. The possibility of $E(^5D_1)$ as the initial state can be safely ruled out from a consideration of the resulting Zeeman patterns. In Sec. IV D, however, we shall show that only $^5D_0$ is important as an initial state.

[8]The A_1 and A_2 no-field states under a magnetic field parallel to the C_4 axis transform like the A representation in C_4. Since L_z transforms as the A representation as well, it is obvious that the diagonal matrix elements $\langle A | L_z | A \rangle$ will give rise to a predominantly first-order Zeeman effect for two closely spaced no-field A_1 and A_2 states.

[9]However, the π and σ polarized spectra shown in

Fig. 11 of Ref. 1 were inadvertently reversed (Ref. 3).

[10]K. W. H. Stevens, Proc. Phys. Soc. (London) A65, 209 (1952).

[11]G. H. Dieke, *Spectra and Energy Levels of Rare Earth Ions in Crystals* (Interscience, New York, 1968), Chap. 10.

[12]G. H. Dieke and R. Sarup, J. Chem. Phys. 36, 371 (1962).

[13]F. K. Fong, L. A. Vredevoe, and R. E. DeWames, Phys. Rev. 170, 412 (1968).

[14]L. A. Vredevoe, C. R. Chilver, and F. K. Fong, in *Progress in Solid State Chemistry*, edited by H. Reiss (Pergamon, New York, to be published), Vol. V.

[15]W. E. Bron and W. R. Heller, Phys. Rev. 136, A1433 (1964).

[16]N. Rabbiner, J. Opt. Soc. Am. 55, 436 (1965).

[17]F. K. Fong, *Progress in Solid State Chemistry*, edited by H. Reiss (Pergamon, New York, 1966), Vol. III, Chap. 4.

PHYSICAL REVIEW B VOLUME 1, NUMBER 11 1 JUNE 1970

Electron Paramagnetic Resonance of Yb^{3+} in Scheelite Single Crystals*

J. P. Sattler and J. Nemarich
Harry Diamond Laboratories, Washington, D. C. 20438
(Received 19 January 1970)

The electron paramagnetic resonance spectra of the ground state of trivalent ytterbium have been observed in eight single crystals with scheelite structure at 4.2 °K and X band frequencies. The crystals used were $CdMoO_4$, $CaWO_4$, $CaMoO_4$, $SrWO_4$, $SrMoO_4$, $PbWO_4$, $PbMoO_4$, and $BaWO_4$. The tetragonal spectra for Yb^{171}, Yb^{173}, and the even isotopes of ytterbium were best fitted with an axial spin Hamiltonian. The g factors were found to have a linear dependence on the crystal c-axis lattice constant. All ground-state wave functions were found to be $\Gamma_{5,6}$. The values of $\langle r^{-3}\rangle$ were calculated for Yb^{3+} in each of the crystals, and all were found to have the value $\langle r^{-3}\rangle = 12.5$ a.u. Inclusion of an orbital reduction factor correction changes this value to $\langle r^{-3}\rangle = 12.8$ a.u.

I. INTRODUCTION

Crystal-field theory has been very useful in describing the qualitative features of the optical spectra of rare-earth ions in solid insulators, but various attempts to account for the magnitude of the crystal-field parameters have been unsuccessful. A review of this situation has been given by Van Vleck.[1] Recently, attempts have been made to improve upon the crystal-field model by considering corrections due to overlap and exchange with ligand ions.[2,3] These calculations indicate that overlap and exchange can make important contributions to the crystal-field parameters, but further work will be necessary before it can be said that quantitative agreement with experiment exists. To provide a body of experimental data which may prove useful in obtaining a better understanding of the strong and weak points of the various theories, an investigation has been conducted at this laboratory of the electron paramagnetic resonance and optical spectra of trivalent ytterbium in a series of isomorphic crystals. The single crystals used for this study were the eight scheelites: cadmium molybdate, barium tungstate, and the molybdates and tungstates of calcium, strontium, and lead. The ytterbium ions appear to be located primarily in undistorted cation sites in these crystals and have tetragonal point symmetry. A good theory should be capable of accounting for the variations observed in the Yb^{3+} spectra as the host crystal-lattice parameters change by approximately 12%.

In this paper, we wish to report on the EPR part of this investigation. The measurements were made at X band and 4.2 °K and fitted to an axial spin Hamiltonian. The g factors were used to calculate the ground-state wave functions for the Yb^{3+} ion in each of the crystals. From the values of the hyperfine parameters for the two isotopes Yb^{171} and Yb^{173}, calculations were made for $\langle r^{-3}\rangle$, the mean inverse cube radius of the Yb^{3+} $4f$ electrons.

II. THEORETICAL CONSIDERATIONS

The EPR spectra of rare-earth ions in various single crystal scheelites have been reported extensively. In particular, studies have been made previously of Yb^{3+} in calcium tungstate,[4,5] lead molybdate,[6] and barium molybdate.[7] In these and other crystals, it was found that the predominant spectra arose from the rare-earth ion in a site with tetragonal point symmetry. This fact, together with chemical arguments based on the valence and ionic size of the rare-earth ions,[8,9] indicates that the rare-earth impurity is located in an undistorted cation site whose point symmetry is S_4.